RSC Advances

COMMUNICATION

View Article Online
View Journal | View Issue

Cite this: *RSC Adv.*, 2015, **5**, 87051

Received 25th June 2015
Accepted 5th October 2015

DOI: 10.1039/c5ra12275a

www.rsc.org/advances

In situ growth of nickel selenide nanowire arrays on nickel foil for methanol electro-oxidation in alkaline media†

Qiong Luo,[ab] Mingying Peng,*[a] Xuping Sun*[b] and Abdullah M. Asiri[c]

In this communication, we develop a simple solvothermal method for *in situ* growth of NiSe nanowire arrays on nickel foil (NiSe/Ni). When used as a 3D anode for electro-catalytic oxidation of methanol in alkaline media, the resulting NiSe/Ni achieves a current density of 132 mA cm^{-2} at 0.5 V (*vs.* SCE) in 1 M KOH with 0.5 M methanol. It retains 88% of the anodic current density after 1000 cyclic voltammetry cycles while the current density can return to 93% of the original value when re-measured in new electrolyte.

Direct methanol fuel cells (DMFCs) have triggered significant attention as sustainable and clean energy devices due to their advantages of high conversion efficiency, low pollutant emission and the availability of methanol fuel.[1,2] However, lowering the costs without loss of the performance is still the main obstacle for the successful commercialization of DMFCs.[3] Compared to acidic DMFCs, alkaline DMFCs have relatively faster kinetics of electro-catalytic oxidation of methanol,[4,5] negligible poisoning effects, increased efficiency, reduced corrosion, and can use non-Pt catalysts.[6] The use of non-Pt catalysts can substantially widen the range of choices for support and catalyst materials, which can reduce the cost of the fuel cell system.

One of the key requirements for alkaline DMFCs is to design efficient and cheap anode catalysts to replace the traditional noble metal catalysts such as Pt and its alloys.[7,8] Therefore, many efforts have recently been devoted to develop non-Pt materials for methanol oxidation like Pd,[9] Ni[10] and other non-noble transition metal oxides.[11,12] Particularly, Ni-based catalysts, such as metal Ni,[10] Ni alloy,[13] $Ni(OH)_2$ (ref. 14) and NiO,[15] are the most widely investigated non-Pt catalysts due to their relatively low cost and high activity. Nickel selenide, an important member of nickel chalcogenides, is a promising material which has a variety of potential applications in Li-ion battery,[16] dye-sensitized solar cell,[17] and electrochemical water splitting.[18] This may be due to the distinctive electronic properties and interesting chemical behaviors of this material.[17] However, to the best of our knowledge, its application for methanol electro-oxidation has not been reported so far.

On the other hand, direct growth of the active phases on the current collectors leads to binder-free catalyst-integrated electrodes. It has been proven to be one effective approach to improve electro-catalytic performance[19,20] because the presence of a polymer binder used for catalyst immobilization may not only increase the series resistance but also block the active sites, leading to decreased catalytic performance.[12,21] Herein, we develop a facile one-step solvothermal approach for *in situ* growth of NiSe nanowire arrays on nickel foil (NiSe/Ni) using NaHSe as Se source and directly use it as a binder-free 3D anode in alkaline DMFCs. This electrode exhibits high catalytic activity and good stability.

The XRD pattern for NiSe/Ni is shown in Fig. 1a. All diffraction peaks marked with triangles can be well indexed to the rhombohedral phase of NiSe (JCPDF: 18-0887)[16] and the peaks marked with asterisks can be assigned to the Ni substrate (JCPDF: 70-1849). No impurity peaks can be detected, suggesting well crystallization and high purity of the product. After solvothermal treatment, the Ni foil (Fig. 1b) was fully covered with NiSe nanowire arrays (Fig. 1c). The nanowires have diameters ranging from 20 to 80 nm with lengths up to several micrometers (Fig. 1d). The transmission electron microscopy (TEM) image (Fig. 1e) shows that the nanowires have a smooth surface. The high-resolution TEM (HRTEM) image reveals well-resolved lattice fringes with interplanar distances of 1.95 Å and 1.64 Å, corresponding to the (131) and (012) planes of NiSe,

[a]*The China-Germany Research Center for Photonic Materials and Devices, The State Key Laboratory of Luminescent Materials and Devices and The Institute of Optical Communication Materials, School of Materials Science and Engineering, South China University of Technology, Guangzhou 510641, China. E-mail: pengmingying@scut.edu.cn*

[b]*State Key Laboratory of Electroanalytical Chemistry, Changchun Institute of Applied Chemistry, Chinese Academy of Sciences, Changchun 130022, Jilin, China. E-mail: sunxp@ciac.ac.cn*

[c]*Chemistry Department, Faculty of Science, King Abdulaziz University, Jeddah 21589, Saudi Arabia*

† Electronic supplementary information (ESI) available: Experimental section and supplementary figures. See DOI: 10.1039/c5ra12275a

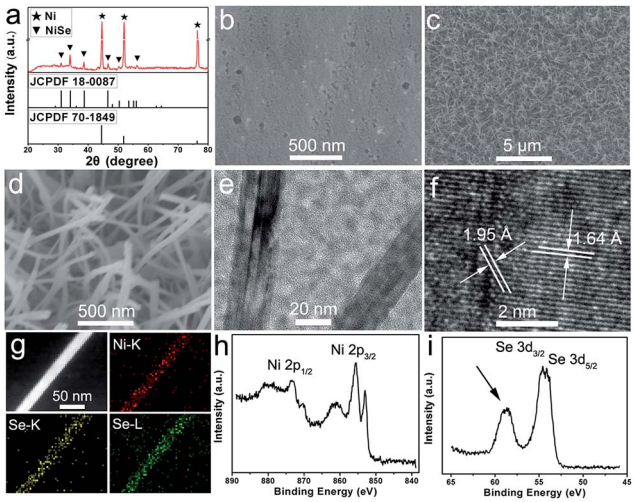

Fig. 1 (a) XRD pattern of NiSe/Ni. SEM images of (b) bare Ni foil and (c and d) NiSe/Ni. (e) TEM and (f) HRTEM images of NiSe nanowire. (g) STEM image and the corresponding EDX elemental mapping images of Ni and Se for NiSe nanowire. XPS spectra in the (h) Ni 2p and (i) Se 3d regions for NiSe/Ni.

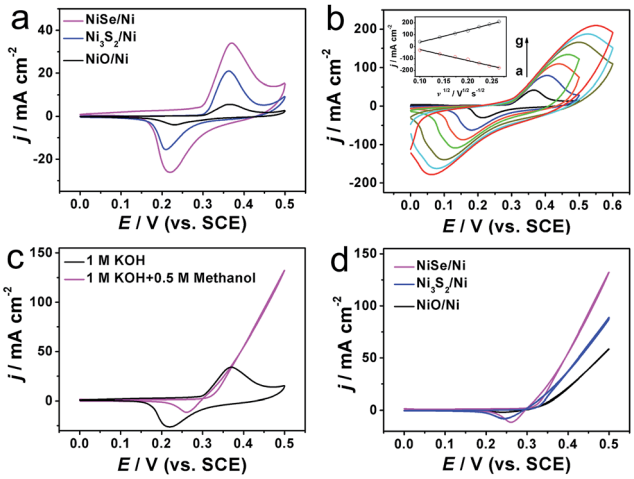

Fig. 2 (a) CV curves of NiSe/Ni, Ni_3S_2/Ni and NiO/Ni in 1 M KOH. (b) CV curves of NiSe/Ni in 1 M KOH at potential sweep rates of 10, 20, 30, 40, 50, 60 and 70 mV s^{-1} (inset: the variation of the peak currents with the square root of scan rate). (c) CV curves of NiSe/Ni in 1 M KOH with and without 0.5 M methanol at a scan rate of 10 mV s^{-1} (d) CV curves of NiSe/Ni, Ni_3S_2/Ni and NiO/Ni in 1 M KOH with 0.5 M methanol at a scan rate of 10 mV s^{-1}.

respectively (Fig. 1e). In addition, the EDX analysis of the product indicates that the atomic ratio of Ni : Se (33.99 : 37.31) is close to the expected 1 : 1 stoichiometry of NiSe, as shown in Fig. S1.† The scanning TEM (STEM) image and the corresponding EDX elemental mapping images of Ni and Se for NiSe nanowire confirm uniform distribution of both Ni and Se elements in the whole nanowire, as shown in Fig. 1f. The composition and chemical valence states of the product were further evaluated by XPS analysis. As shown in Fig. 1g, the Ni $2p_{3/2}$ and Ni $2p_{1/2}$ peaks appearing at 855.6 eV and 873.5 eV, respectively, correspond to Ni^{2+}.[22] The peaks at 853.0 eV and 870.3 eV can be attributed to metallic Ni 2p arising from the Ni substrate.[23] The binding energy of Se 3d (Fig. 1h) at 54.4 eV suggests the presence of Se^{2-},[22] while the weaker shoulder peaks (shown by arrows in Fig. 1h) may result from the oxidation of Se^{2-} ions on the surface of the product.[24] All these structure and composition characterizations demonstrate that NiSe nanowire arrays was directly grow on Ni foil through a simple solvothermal process.

We probed the catalytic performance of the 3D NiSe/Ni electrode toward electro-catalytic oxidation of methanol. For comparison, NiO nanowires on Ni foil (NiO/Ni) and Ni_3S_2 nanowires on Ni foil (Ni_3S_2/Ni) were also studied (Fig. S2 and S3†). Fig. 2a presents the cyclic voltammetry (CV) curves of NiSe/Ni, Ni_3S_2/Ni and NiO/Ni electrodes in 1 M KOH electrolyte. All these three electrodes exhibit a pair of distinct redox peaks, respectively, which can be ascribed to the reversible reaction between Ni^{2+}/Ni^{3+} in alkaline media.[15,25] The CV curves of NiSe/Ni show much higher peak current and larger enclosed area compared with NiO/Ni and Ni_3S_2/Ni electrodes, indicating that NiSe/Ni has much better electrochemical performance. Fig. 2b shows the CV curves of NiSe/Ni electrode in 1 M KOH at different potential sweep rates. Both anodic and cathodic peak currents increase with scan rate, meanwhile, the anodic peak potential displays a positive shift and the cathodic peak potential has a negative shift with increased scan rate. Additionally, the linear relationships of the peak currents *versus* the square roots of scan rate ($v^{1/2}$) can be observed (Fig. 2b inset). The above results demonstrate that the electrochemical formation of Ni^{3+} from Ni^{2+} is a diffusion-controlled process.[26]

The methanol electro-catalytic oxidation property on NiSe/Ni is shown in Fig. 2c. Comparing the CV curves in 1 M KOH with and without methanol, the electro-oxidation of methanol on the NiSe/Ni electrode is clearly observed and a sharp increase in anodic current for methanol oxidation is noticed. Compared with the NiO/Ni and Ni_3S_2/Ni electrodes, the NiSe/Ni electrode has a much higher activity for methanol oxidation (Fig. 2d), which affords 132 mA cm^{-2} at 0.5 V. Moreover, the activity of bare Ni foil for methanol oxidation is poor as shown in Fig. S4.† Furthermore, the onset of oxidation potential for our NiSe/Ni anode is shifted to a more negative potential (from 0.31 to 0.35 V) compared to Ni foil, indicating a better kinetic performance for methanol oxidation. Nevertheless, the onset potential of NiSe/Ni is still higher than well-known noble metal electrocatalysts.[27,28] Given Se, O, and S elements are in the same family with similar properties, we may suggest that NiSe/Ni electrode shares similar methanol oxidation mechanism with nickel oxide or sulfide.[29,30] Note that the NiSe/Ni electrode also outperforms some previously reported catalysts including $NiCo_2O_4$,[19] $NiCo_2S_x$,[29] titanium-supported nano-scale Ni flakes,[31] and NiO/multi-walled carbon nanotubes composites.[32] The high electro-catalytic activity of NiSe/Ni could be attributed to the following four reasons. (1) The high electrical conductivity of NiSe[16] favors fast electron transport along it. (2) The direct growth of NiSe on Ni substrate ensures intimate contact, good mechanical adhesion and excellent electrical connection between them.[20] (3) The nanowire arrays is capable of vectorial

electron transport and the open spaces between the nanowires allow for better diffusion of electrolyte and methanol as well as more efficient utilization of active sites.[33] (4) The binder-free nature for this electrode leads to improved conductivity[21] and effectively avoids blocking of active sites and the inhibition of diffusion.[34]

Electrochemical impedance spectroscopy (EIS) is an effective tool for studying the electrochemical properties of the electrode. EIS measurements were recorded at 0.5 V with a frequency range of 100 kHz to 0.1 Hz at an AC amplitude of 5 mV. Fig. 3 shows the Nyquist plots of the NiSe/Ni, Ni_3S_2/Ni and NiO/Ni electrodes in 1 M KOH with 0.5 M methanol. The primary semicircle in the Nyquist plot is attributed to the charge-transfer resistance, which is related to the electro-catalytic kinetics and a smaller semicircle corresponds to a smaller charge transfer resistance.[35] The charge-transfer resistance of the NiSe/Ni electrode is the smaller than Ni_3S_2/Ni and NiO/Ni electrodes; therefore, NiSe/Ni shows the best electro-catalytic kinetics for methanol oxidation, which is consistent with the result obtained from CV curves (Fig. 2d).

We also probed the stability of NiSe/Ni electrode by continuous CV scanning. As shown in Fig. 4a, this electrode retains 88% of the anodic current density at 0.5 V after 1000 CV cycles. The same electrode was washed repeatedly and reused in the oxidation of methanol with a fresh electrolyte. In this case, the current density can return to 93% of the original value. Thus, this result demonstrates that the observed current decay with successive potential scans may partly due to the consumption of methanol. These results suggest that our proposed NiSe/Ni has good long-term stability for the electro-catalytic oxidation of methanol.

As shown in Fig. S5,† the size of semicircle at 0.5 V is much smaller than that at 0.4 V, suggesting that the lower electron or charge transfer resistance and the faster reaction kinetics for methanol oxidation at 0.5 V, so 0.5 V was selected as the optimal potential for further investigating the long-term stability of NiSe/Ni electrode for methanol oxidation. Fig. 4b presents the chronoamperometry (CA) curves for NiSe/Ni, Ni_3S_2/Ni, NiO/Ni and bare Ni foil in 1 M KOH with 0.5 M methanol at 0.5 V. As observed, Ni_3S_2/Ni, NiO/Ni and bare Ni foil display obviously current degradation after 20 000 s electrolysis, while NiSe/Ni shows nearly no decay and exhibits the highest current density, suggesting its good long-term electrochemical stability. The high electro-catalytic activity and good stability of NiSe/Ni electrode imply its potential application in alkaline DMFCs.

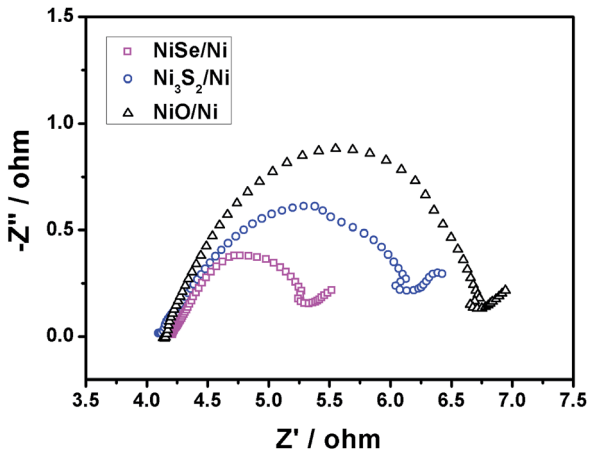

Fig. 3 EIS plots of NiSe/Ni, Ni_3S_2/Ni and NiO/Ni electrodes in 1 M KOH with 0.5 M methanol at 0.5 V.

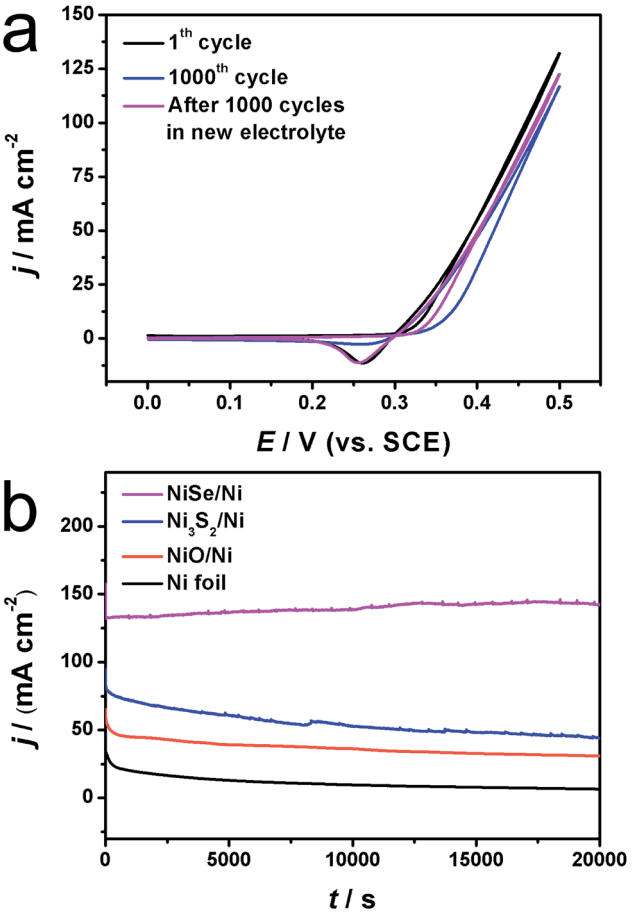

Fig. 4 (a) CV curves of NiSe/Ni electrode in 1 M KOH with 0.5 M methanol at a scan rate of 10 mV s^{-1} before and after 1000 CV cycles. (b) CA curves of NiSe/Ni, Ni_3S_2/Ni, NiO/Ni and bare Ni foil in 1 M KOH with 0.5 M methanol at 0.5 V.

In summary, NiSe nanowire arrays have been *in situ* solvothermally grown on nickel foil. When used as a binder-free 3D electrode in alkaline DMFCs, the resulting NiSe/Ni architecture shows high performance toward methanol electro-oxidation. The superior catalytic activity and stability, along with the simple and scalable fabrication process, of this 3D electrode offer promising features for use as a cheap catalyst material toward electro-oxidation of methanol and other organic small molecules.

Acknowledgements

This work was supported by the National Natural Science Foundation of China (Grant no. 51322208), the Guangdong Natural Science Foundation for Distinguished Young Scholars

(Grant no. S20120011380), the Department of Education of Guangdong Province (Grant no. 2013gjhz0001), Fundamental Research Funds for the Central Universities, the National Natural Science Foundation of China (no. 21175129) and the National Basic Research Program of China (no. 2011CB935800).

Notes and references

1 M. Winter and R. J. Brodd, *Chem. Rev.*, 2004, **104**, 4245.
2 K. M. McGrath, G. K. S. Prakash and G. A. Olah, *J. Ind. Eng. Chem.*, 2004, **10**, 1063.
3 H. Li, S. Zhao, M. Gong, C. Cui, D. He, H. Liang and S. Yu, *Angew. Chem.*, 2013, **125**, 7620.
4 J. H. Kim, H. K. Kim, K. T. Hwang and J. Y. Lee, *Int. J. Hydrogen Energy*, 2010, **35**, 768.
5 E. Antolini and E. R. Gonzalez, *J. Power Sources*, 2010, **195**, 3431.
6 F. Bidault, D. J. L. Brett, P. H. Middleton and N. P. Brandon, *J. Power Sources*, 2009, **187**, 39.
7 W. Yuan, Y. Cheng, P. Shen, C. Li and S. Jiang, *J. Mater. Chem. A*, 2015, **3**, 1961.
8 B. Xia, H. Wu, X. Wang and X. Lou, *J. Am. Chem. Soc.*, 2012, **134**, 13934.
9 H. Li, G. Chang, Y. Zhang, J. Tian, S. Liu, Y. Luo, A. M. Asiri, A. O. Al-Youbi and X. Sun, *Catal. Sci. Technol.*, 2012, **2**, 1153.
10 M. A. A. Rahim, R. M. A. Hameed and M. W. Khalil, *J. Power Sources*, 2004, **134**, 160.
11 Y. Zhao, S. Nie, H. Wang, J. Tian, Z. Ning and X. Li, *J. Power Sources*, 2012, **218**, 320.
12 J. Wu, Z. Li, X. Huang and Y. Lin, *J. Power Sources*, 2013, **224**, 1.
13 I. Danaee, M. Jafarian, A. Mirzapoor, F. Gobal and M. G. Mahjani, *Electrochim. Acta*, 2010, **55**, 2093.
14 A. A. El-Shafei, *J. Electroanal. Chem.*, 1999, **471**, 89.
15 X. Tong, Y. Qin, X. Guo, O. Moutanabbir, X. Ao, E. Pippel, L. Zhang and M. Knez, *Small*, 2012, **8**, 3390.
16 L. Mi, H. Sun, Q. Ding, W. Chen, C. Liu, H. Hou and C. Shen, *Dalton Trans.*, 2012, 12595.
17 F. Gong, H. Wang, X. Xu, G. Zhou and Z. Wang, *J. Am. Chem. Soc.*, 2012, **134**, 10953.
18 M. Gao, Z. Lin, T. Zhuang, J. Jiang, Y. Xu, Y. Zheng and S. Yu, *J. Mater. Chem.*, 2012, **22**, 13662.
19 L. Qian, L. Gu, L. Yang, H. Yuan and D. Xiao, *Nanoscale*, 2013, **5**, 7388.
20 J. Tian, Q. Liu, A. M. Asiri and X. Sun, *J. Am. Chem. Soc.*, 2014, **136**, 7587.
21 Y. Luo, J. Jiang, W. Zhou, H. Yang, J. Luo, X. Qi, H. Zhang, D. Y. W. Yu, C. Li and T. Yu, *J. Mater. Chem.*, 2012, **22**, 8634.
22 W. Shi, X. Zhang and G. Che, *Int. J. Hydrogen Energy*, 2013, **38**, 7037.
23 P. Prieto, V. Nistor, K. Nouneh, M. Oyama, M. Abd-Lefdil and R. Díaz, *Appl. Surf. Sci.*, 2012, **258**, 8807.
24 X. Liu, X. Duan and P. Peng, *Nanoscale*, 2011, **3**, 5090.
25 H. Chen, J. Li, C. Long, T. Wei, G. Ning, J. Yan and Z. Fan, *J. Mar. Sci. Appl.*, 2014, **13**, 462.
26 S. N. Azizi, S. Ghasemi and E. Chiani, *Electrochim. Acta*, 2013, **88**, 463.
27 K. Jeremy and W. A. Goddard, *J. Am. Chem. Soc.*, 1999, **121**, 10928.
28 H. Wang, Z. Sun, Y. Yang and D. Su, *Nanoscale*, 2013, **5**, 139.
29 L. Qian, W. Chen, R. Huang and D. Xiao, *RSC Adv.*, 2015, **5**, 4092.
30 N. Spinner and W. E. Mustain, *Electrochim. Acta*, 2011, **56**, 5656.
31 Q. Yi, W. Huang, J. Zhang, X. Liu and L. Li, *Catal. Commun.*, 2008, **9**, 2053.
32 M. Asgari, M. G. Maragheh, R. Davarkhah and E. Lohrasbi, *J. Electrochem. Soc.*, 2011, **158**, K225.
33 P. Jiang, Q. Liu, Y. Liang, J. Tian, A. M. Asiri and X. Sun, *Angew. Chem., Int. Ed.*, 2014, **53**, 12855.
34 J. D. Roy-Mayhew, G. Boschloo, A. Hagfeldt and I. A. Aksay, *ACS Appl. Mater. Interfaces*, 2012, **4**, 2794.
35 L. Xia, P. Guo, Y. Wang, S. Ding and J. He, *J. Power Sources*, 2014, **262**, 232.

